

Supporting Information

Table of Contents

Page No.

Additional Experimental Details

1. Sample Preparation.	2
2. PXRD Measurements and Analysis.	2
3. DSC Measurements and Analysis.	2
4. SXD Measurements and Analysis.	3

List of Tables

SXD data on phase I of C₆H₃(CH₃)₃:C₆F₆.	
Table S1a. Crystal data and structure refinement.	4
Table S1b. Fractional atomic coordinates and U(eq) for all atoms.	5
Table S1c. Anisotropic displacement parameters.	5
Table S1d. Selected bond lengths.	6
Table S1e. Selected bond angles.	6
SXD data on phase II of C₆H₃(CH₃)₃:C₆F₆.	
Table S2a. Crystal data and structure refinement.	7
Table S2b. Fractional atomic coordinates and U(eq) for all atoms.	8
Table S2c. Anisotropic displacement parameters.	9
Table S2d. Selected bond lengths.	10
Table S2e. Selected bond angles.	10
SXD data on phase III of C₆H₃(CH₃)₃:C₆F₆.	
Table S3a. Crystal data and structure refinement.	11
Table S3b. Fractional atomic coordinates and U(eq) for all atoms.	12
Table S3c. Anisotropic displacement parameters.	14
Table S3d. Selected bond lengths.	15
Table S3e. Selected bond angles.	16
PXRD data on phases I to III of C₆H₃(CH₃)₃:C₆F₆.	
Table S4. Lattice parameters derived from the PXRD data.	17

List of Figures

Figure S1. PXRD data of C ₆ H ₃ (CH ₃) ₃ :C ₆ F ₆ .	18
Figure S2. DSC data of pure C ₆ H ₃ (CH ₃) ₃ .	19
Figure S3. PXRD data of C ₆ H ₃ (CH ₃) ₃ :C ₆ F ₆ measured with a CCD detector.	20
Figure S4. PXRD data of two samples of C ₆ H ₃ (CH ₃) ₃ :C ₆ F ₆ at 100 K.	21
Figure S5. Reciprocal space data for the 3 phases of C ₆ H ₃ (CH ₃) ₃ :C ₆ F ₆ .	22
Figure S6. Single crystals of C ₆ H ₃ (CH ₃) ₃ :C ₆ F ₆ .	23
Figure S7. Labelling of the atoms for the crystal structures of phases I, II, and III.	24
Figure S8. Crystal structures of phases I-III viewed down the b-axis.	25
Figure S9. –F...H ₃ C– interaction in C ₆ H ₃ (CH ₃) ₃ :C ₆ F ₆ phase II viewed down the a-axis.	26
Figure S10. Lattice parameter data derived from PXRD data shown in Figure 1.	27

Additional Experimental Details

1. Sample Preparation

1.86 g of hexafluorobenzene (Aldrich H8706, 25 g, MW=186.05, 99%) were added to 1.20 g of mesitylene (Aldrich M720-0, 500 mL, MW=120.2, Gold Label >99%) in a small sealable bottle. Given the antiquity of the bottle of mesitylene, ^1H NMR was used to confirm that the purity of the mesitylene (stored over MgSO_4) was > 99%. The sealed bottle was gently heated in warm water (40-50 °C) to dissolve the solids and ensure complete mixing of the liquid components and then left at ambient temperature to solidify. Material stored in the glass bottle sublimed with time into large single crystals; crystals from this bottle were used for SXD experiments. Even at room temperature, the solid adduct formed within the bottle was surprisingly hard making single crystals difficult to extract.

2. PXRD Measurements and Analysis

The binary adduct was melted by heating the sealed bottle in warm water (40-50 °C) and a small amount of liquid was pipetted into the neck of a 1 mm X-ray capillary held in the same warm water. The liquid was shaken to the end of the capillary, which was subsequently flame sealed. Several variable temperature PXRD measurements were performed using a Stoe Stadi-P diffractometer equipped with a Cu anode, $\text{Ge}<111>$ monochromator, a Dectris Mythen 1K detector, and an Oxford Instruments CryojetHT (90-500 K) with an in-house modified sample setup. Measurements were made on cooling from 300 K (shown in Figure 1 and Figure S1) and on heating from 90 K, both in 10 K intervals. The detector was scanned in 2θ from 2° to 60° in steps of 0.5° at 10 s per step, a complete scan lasting approx. 30 min and each 10 K temperature change took approx. 12-15 min.

Lattice parameters were obtained as a function of temperature (shown in Figure 5 and Figure S10) by Le Bail whole pattern fitting with a pseudo-Voigt peak shape using the program Rietica version 1.77 [B. A. Hunter, 1997]. Background count was estimated graphically, and the total number of parameters fitted was 6 for phases I and III and 7 for phase II, with just 3 parameters being used for peak width and shape.

3. DSC Measurements

19.3 mg of $\text{C}_6\text{H}_3(\text{CH}_3)_3:\text{C}_6\text{F}_6$ was crimped into an aluminum sample pan and loaded into the DSC8000 calorimeter at +20 °C. The sample was held at +20 °C for 1 min and then cooled at 10 °C min^{-1} to -150 °C. The sample was then held at -150 °C for 1 min and subsequently cooled to -180 °C at the slower rate of 2 °C min^{-1} (data not shown in Figure 2). A slower heating rate was required at low temperatures to allow for a decrease in the cooling power of the cold stage. The sample was held at the lowest temperature for 3 min, and then heated to +60 °C at 10 °C min^{-1} . The experiment was stopped once the sample had started to melt at around +34 °C. Thermal transitions were observed on cooling at -71.71 °C ($\Delta H = -4.8 \text{ J g}^{-1}$), -94.77 °C ($\Delta H = -0.24 \text{ J g}^{-1}$), and -163.71 °C ($\Delta H = -0.44 \text{ J g}^{-1}$) and on heating at -160.63 °C ($\Delta H = 0.64 \text{ J g}^{-1}$), -93.18 °C ($\Delta H = 0.22 \text{ J g}^{-1}$), and -56.29 °C ($\Delta H = 5.0 \text{ J g}^{-1}$).

The experiment was repeated using the same scan details but with pure mesitylene $\text{C}_6\text{H}_3(\text{CH}_3)_3$ (using a near identical mass of 19.3 mg). The sample was observed to freeze

very sharply at $-69.58\text{ }^{\circ}\text{C}$ ($\Delta H = 52\text{ J g}^{-1}$) and to melt slowly at around $-45.13\text{ }^{\circ}\text{C}$ ($\Delta H = -57\text{ J g}^{-1}$). An additional weak transition was observed on heating at $-81.08\text{ }^{\circ}\text{C}$ ($\Delta H = 0.85\text{ J g}^{-1}$). The data are shown in Figure S2. Finally, the first experiment on $\text{C}_6\text{H}_3(\text{CH}_3)_3:\text{C}_6\text{F}_6$ was repeated (sample mass 18.9 mg) and similar results were obtained. Thermal transitions were observed on cooling at $-87.71\text{ }^{\circ}\text{C}$ ($\Delta H = -3.2\text{ J g}^{-1}$), $-94.84\text{ }^{\circ}\text{C}$ ($\Delta H = -0.16\text{ J g}^{-1}$), and $-163.56\text{ }^{\circ}\text{C}$ ($\Delta H = -0.50\text{ J g}^{-1}$) and on heating at $-160.37\text{ }^{\circ}\text{C}$ ($\Delta H = 0.73\text{ J g}^{-1}$), $-93.07\text{ }^{\circ}\text{C}$ ($\Delta H = 0.20\text{ J g}^{-1}$), and $-55.29\text{ }^{\circ}\text{C}$ ($\Delta H = 3.6\text{ J g}^{-1}$). All values were determined using the Pyris software package (version 11.1.1.0492) from PerkinElmer.

4. SXD Measurements and Analysis

Single crystals of $\text{C}_6\text{H}_3(\text{CH}_3)_3:\text{C}_6\text{F}_6$ were held in a Hampton Research nylon loop (20 μm thickness, 0.9 mm diameter, shown in Figure S6). Measurements were made on crystals at 190 K (phase I), 150 K (phase II), and 100 K (phase III) using a twin-source SuperNova diffractometer with a micro-focus Cu X-ray beam (50 kV, 0.8 mA), an Atlas (135 mm CCD) detector, and the sample temperature was controlled with an Oxford Instruments Cryojet5. Full spheres of data were collected for phases II and III, and a half sphere for phase I. The data were processed with the CrysAlisPro software package (version 1.171.38.43) from Rigaku Oxford Diffraction. Crystal structures of each phase were solved and refined by least-squares within the Olex2 program suite [O. V. Dolomanov, L. J. Bourhis, R. J. Gildea, J. A. K. Howard, H. Puschmann, *J. Appl. Crystallogr.* 2009, **42**, 339-341.] using the ShelXS structure solution program and the ShelXL 2014 refinement program [G. M. Sheldrick, *Acta Crystallogr.* 2015, **C71**, 3-8.]. The positions of all of the hydrogen atoms in each phase were clearly identified as the strongest peaks in Fourier difference maps.

In phase III, the hydrogen atoms on the ring were constrained with the ShelXL AFIX 43 instruction and those of the methyl groups with the AFIX 137 instruction. In addition, an automatic restraint was applied to fix the origin in y as required for the polar space-group $Pb2(1)a$. The use of a non-standard setting and origin (so as to match the description of the structure of phase II) demonstrated several bugs in various crystallographic software, and in particular with the IUCr program CheckCIF which was unable to recognise the space group from the symmetry operators. For phase II, the data exhibited micro-domain twinning due to the monoclinic symmetry (Figure S5) and were processed as twinned in CrysAlisPro and refined in ShelXL as a 49.4%:50.6% twin with HKLF set to 5. The hydrogen atoms on the ring and those of the methyl groups were constrained as for phase III, but with two of the three methyl groups disordered. In phase I, the hydrogen atoms on the ring were constrained with the ShelXL AFIX 43 instruction but the disordered hydrogen atoms of the methyl groups were restrained with DFIX and SADI instructions with values equivalent to an AFIX 137 instruction. Further details on all three structures are provided in the summary tables below (Tables S1a-e to S3a-e).

Table S1a. Crystal data and structure refinement for phase I of C₆H₃(CH₃)₃:C₆F₆.

Identification code	xstr0591a
Empirical formula	C ₁₅ H ₁₂ F ₆
Formula weight	306.25
Temperature / K	190
Crystal system	orthorhombic
Space group	Pbnm [†]
a / Å	7.08543(18)
b / Å	15.3044(4)
c / Å	13.2959(4)
α / °	90
β / °	90
γ / °	90
Volume / Å ³	1441.79(6)
Z	4
ρ _{calc} / g cm ⁻³	1.411
μ / mm ⁻¹	1.205
F(000)	624.0
Crystal size / mm ³	0.887 × 0.596 × 0.429
Radiation	CuKα ($\lambda = 1.54184$)
2θ range for data collection / °	13.772 to 147.232
Index ranges	-8 ≤ h ≤ 6, -19 ≤ k ≤ 17, -16 ≤ l ≤ 16
Reflections collected	11235
Independent reflections	1505 [$R_{\text{int}} = 0.0265$, $R_{\text{sigma}} = 0.0117$]
Data/restraints/parameters	1505/49/128
Goodness-of-fit on F^2	1.105
Final R indexes [$I \geq 2\sigma(I)$]	$R_1 = 0.0670$, $wR_2 = 0.2130$
Final R indexes [all data]	$R_1 = 0.0720$, $wR_2 = 0.2221$
Largest diff. peak/hole / e Å ⁻³	0.18/-0.22

[†]Space group Pnma with the axes labels permuted so as to match the space group setting used for phase II and with columns of molecules stacked along a. A standard origin is used.

Table S1b. Fractional atomic coordinates ($\times 10^4$) and equivalent isotropic displacement parameters ($\text{\AA}^2 \times 10^3$) for phase I of $\text{C}_6\text{H}_3(\text{CH}_3)_3:\text{C}_6\text{F}_6$. U_{eq} is defined as $\frac{1}{3}$ of the trace of the orthogonalised U_{ij} tensor.

Atom	x	y	z	$U(\text{eq})$
C(1)	8494(3)	5097.6(18)	6987(3)	123.7(12)
C(2)	8810(3)	4331(2)	6471(2)	102.6(9)
C(3)	9122(3)	3583.3(14)	6992.7(16)	82.3(7)
F(1)	8173(4)	5835.3(14)	6490(3)	210.1(14)
F(2)	8789(3)	4313.0(17)	5475.3(16)	174.9(12)
F(3)	9413(3)	2837.5(11)	6500.6(11)	118.3(7)
C(4)	5768(3)	6773.5(15)	2500	71.7(7)
C(5)	5930(2)	6343.4(13)	3407.8(15)	74.7(6)
C(6)	6275(3)	5452.8(13)	3394.3(16)	77.7(6)
C(7)	6447(3)	4995.2(16)	2500	77.1(8)
C(8)	6789(6)	4025.0(19)	2500	125.6(16)
C(9)	5744(4)	6837(2)	4389(2)	120(1)
H(4)	5539	7385	2500	86
H(6)	6396	5148	4013	93
H(8A)	5781(7)	3739(2)	2836.8(4)	188
H(8B)	6861(7)	3820(2)	1826.6(9)	188
H(8C)	7941(6)	3902(3)	2837.0(18)	188
H(9A)	6849(12)	7175(10)	4500(8)	180
H(9B)	4677(16)	7212(9)	4358(6)	180
H(9C)	5590(30)	6433(3)	4926(3)	180
H(9D)	6731(17)	6667(11)	4831(6)	180
H(9E)	5820(30)	7446.5(19)	4264(4)	180
H(9F)	4560(13)	6706(11)	4689(8)	180

Table S1c. Anisotropic displacement parameters ($\text{\AA}^2 \times 10^3$) for phase I of $\text{C}_6\text{H}_3(\text{CH}_3)_3:\text{C}_6\text{F}_6$. Anisotropic displacement factor exponent has the form: $-2\pi^2[h^2a^{*2}U_{11}+2hka^{*}b^{*}U_{12}+\dots]$.

Atom	U_{11}	U_{22}	U_{33}	U_{23}	U_{13}	U_{12}
C(1)	74.5(13)	95.3(16)	201(3)	41.7(18)	-10.1(14)	8.2(10)
C(2)	85.2(14)	116(2)	107.1(18)	27.5(14)	-8.6(11)	-8.2(12)
C(3)	71.8(11)	86.8(13)	88.2(13)	0.1(10)	0.1(8)	-8.5(8)
F(1)	158.4(19)	122.4(15)	349(4)	97(2)	-26.3(19)	23.6(12)
F(2)	198(2)	210(3)	116.8(15)	67.7(15)	-21.1(12)	-25.8(15)
F(3)	148.2(14)	104.1(12)	102.5(11)	-22.8(8)	3.8(8)	-8.4(9)
C(4)	62.3(12)	54.1(12)	98.6(18)	0	0	-3.0(9)
C(5)	64.2(10)	73.0(11)	86.8(13)	-7.9(8)	3.7(7)	-6.6(7)
C(6)	68.9(10)	73.8(12)	90.4(13)	16.3(9)	-1.6(8)	-5.8(8)
C(7)	59.7(13)	55.9(13)	116(2)	0	0	-1.6(9)
C(8)	111(2)	54.7(15)	212(5)	0	0	5.3(15)
C(9)	125(2)	132(2)	102.8(18)	-36.0(17)	10.1(15)	-7.6(16)

Table S1d. Selected bond lengths for phase I of C₆H₃(CH₃)₃:C₆F₆.

Atom — Atom	Length / Å	Atom — Atom	Length / Å
C(1) — C(1) ¹	1.365(7)	C(4) — C(5)	1.380(2)
C(1) — C(2)	1.378(4)	C(4) — C(5) ²	1.380(2)
C(1) — F(1)	1.328(3)	C(5) — C(6)	1.385(3)
C(2) — C(3)	1.356(4)	C(5) — C(9)	1.513(3)
C(2) — F(2)	1.324(4)	C(6) — C(7)	1.385(3)
C(3) — C(3) ¹	1.349(4)	C(7) — C(6) ²	1.385(3)
C(3) — F(3)	1.332(3)	C(7) — C(8)	1.504(4)

¹x, y, 1½ – z and ²x, y, ½ – z

Table S1e. Selected bond angles for phase I of C₆H₃(CH₃)₃:C₆F₆.

Atom — Atom — Atom	Angle / °	Atom — Atom — Atom	Angle / °
C(1) ¹ — C(1) — C(2)	119.84(17)	C(5) — C(4) — C(5) ²	122.1(2)
F(1) — C(1) — C(1) ¹	119.8(2)	C(4) — C(5) — C(6)	118.22(18)
F(1) — C(1) — C(2)	120.3(3)	C(4) — C(5) — C(9)	120.6(2)
C(3) — C(2) — C(1)	119.4(3)	C(6) — C(5) — C(9)	121.2(2)
F(2) — C(2) — C(1)	120.9(3)	C(5) — C(6) — C(7)	121.61(18)
F(2) — C(2) — C(3)	119.7(3)	C(6) — C(7) — C(6) ²	118.3(2)
C(3) ¹ — C(3) — C(2)	120.76(17)	C(6) — C(7) — C(8)	120.87(12)
F(3) — C(3) — C(2)	119.8(2)	C(6) ² — C(7) — C(8)	120.87(12)
F(3) — C(3) — C(3) ¹	119.43(12)		

¹x, y, 1½ – z and ²x, y, ½ – z

Table S2a. Crystal data and structure refinement for phase II of C₆H₃(CH₃)₃:C₆F₆.

Identification code	xstr0634_twin1_hklf5
Empirical formula	C ₁₅ H ₁₂ F ₆
Formula weight	306.25
Temperature / K	150
Crystal system	monoclinic
Space group	P2 ₁ /n
<i>a</i> / Å	7.0737(3)
<i>b</i> / Å	15.2833(5)
<i>c</i> / Å	13.2104(4)
α / °	90
β / °	96.629(3)
γ / °	90
Volume / Å ³	1418.61(8)
<i>Z</i>	4
ρ_{calc} / g cm ⁻³	1.434
μ / mm ⁻¹	1.225
<i>F</i> (000)	624.0
Crystal size / mm ³	0.554 × 0.356 × 0.277
Radiation	CuKα (λ = 1.54184)
2θ range for data collection / °	8.882 to 147.272
Index ranges	-8 ≤ <i>h</i> ≤ 8, -18 ≤ <i>k</i> ≤ 18, -16 ≤ <i>l</i> ≤ 16
Reflections collected	5797
Independent reflections	5797 [R _{int} = 0.0578, R _{sigma} = 0.0238]
Data/restraints/parameters	5797/0/194
Goodness-of-fit on <i>F</i> ²	1.082
Final <i>R</i> indexes [<i>I</i> >= 2σ(<i>I</i>)]	<i>R</i> ₁ = 0.0687, <i>wR</i> ₂ = 0.2017
Final <i>R</i> indexes [all data]	<i>R</i> ₁ = 0.0721, <i>wR</i> ₂ = 0.2054
Largest diff. peak/hole / e Å ⁻³	0.34/-0.32

Table S2b. Fractional atomic coordinates ($\times 10^4$) and equivalent isotropic displacement parameters ($\text{\AA}^2 \times 10^3$) for phase II of $\text{C}_6\text{H}_3(\text{CH}_3)_3:\text{C}_6\text{F}_6$. U_{eq} is defined as $\frac{1}{3}$ of the trace of the orthogonalised U_{ij} tensor.

Atom	x	y	z	U(eq)
C(1)	848(3)	6409.2(14)	2949.5(16)	52.6(5)
C(2)	959(3)	6408.1(16)	1929.6(17)	57.1(6)
C(3)	1307(3)	5649(2)	1449(2)	72.7(8)
C(4)	1526(3)	4877(2)	2005(3)	87.6(11)
C(5)	1408(4)	4895.2(19)	3037(3)	81.6(9)
C(6)	1075(3)	5660.0(18)	3506(2)	65.4(6)
F(1)	530(2)	7159.5(10)	3425.1(12)	78.7(5)
F(2)	750(3)	7156.8(12)	1415.3(13)	93.2(6)
F(3)	1449(3)	5653.0(18)	452.3(14)	122.5(9)
F(4)	1868(3)	4132.2(15)	1533(3)	154.8(13)
F(5)	1647(4)	4151.9(13)	3571(3)	147.7(12)
F(6)	982(3)	5685.4(15)	4505.8(14)	106.9(7)
C(7)	4118(3)	3629.7(14)	6662.9(17)	50.9(5)
C(8)	3793(3)	4524.9(14)	6620.8(17)	53.3(5)
C(9)	3575(3)	5004.5(13)	7495.5(18)	52.9(5)
C(10)	3686(3)	4568.3(14)	8418.5(17)	51.3(5)
C(11)	4011(3)	3674.3(14)	8485.1(16)	50.2(5)
C(12)	4227(3)	3220.6(12)	7598.9(16)	49.6(5)
C(13)	4341(4)	3115(2)	5706(2)	81.1(8)
C(14)	3246(5)	5976.5(16)	7439(3)	89(1)
C(15)	4131(5)	3203(2)	9495(2)	83.2(9)
H(8)	3719	4816	5982	64
H(10)	3536	4889	9020	62
H(12)	4457	2608	7636	59
H(13A)	4613	3518	5163	122
H(13B)	3161	2796	5491	122
H(13C)	5393	2699	5843	122
H(13D)	4267	2488	5850	122
H(13E)	5578	3249	5476	122
H(13F)	3322	3276	5171	122
H(14A)	2612	6165	8023	133
H(14B)	2443	6119	6806	133
H(14C)	4471	6279	7450	133
H(15A)	3140	3425	9889	125
H(15B)	5385	3305	9876	125
H(15C)	3946	2574	9377	125
H(15D)	5069	2730	9506	125
H(15F)	2883	2957	9588	125
H(15E)	4519	3616	10048	125

Table S2c. Anisotropic displacement parameters ($\text{\AA}^2 \times 10^3$) for phase II of $\text{C}_6\text{H}_3(\text{CH}_3)_3:\text{C}_6\text{F}_6$. Anisotropic displacement factor exponent has the form: $-2\pi^2[h^2a^{*2}U_{11}+2hka^{*}b^{*}U_{12}+\dots]$.

Atom	U_{11}	U_{22}	U_{33}	U_{23}	U_{13}	U_{12}
C(1)	46.8(10)	57.6(11)	53.4(12)	1.4(9)	6.2(9)	-4.0(9)
C(2)	52.3(11)	66.8(13)	51.8(12)	4.5(10)	3.9(9)	-12.3(10)
C(3)	48.1(12)	106(2)	65.6(14)	-26.7(15)	13.9(10)	-13.8(13)
C(4)	44.3(13)	71.4(17)	147(3)	-44(2)	10.6(15)	4.2(11)
C(5)	57.5(14)	63.0(15)	122(3)	17.9(16)	1.5(15)	5.2(11)
C(6)	53.9(12)	76.1(16)	66.4(14)	17.7(12)	8.4(10)	-3.2(11)
F(1)	91.6(11)	70.0(9)	73.6(10)	-17.6(7)	6.3(8)	2.1(8)
F(2)	118.6(14)	89.8(12)	68.8(10)	29.2(8)	0.2(9)	-21(1)
F(3)	98.9(14)	202(3)	70.8(11)	-58.3(13)	26.8(10)	-34.0(14)
F(4)	90.4(14)	108.6(16)	263(3)	-102(2)	9.8(17)	18.8(11)
F(5)	128.4(19)	74.3(12)	232(3)	59.3(16)	-16.0(19)	12.6(12)
F(6)	113.7(15)	141.7(18)	65.4(10)	39.7(11)	11.2(9)	-11.5(13)
C(7)	42.3(10)	53.2(11)	57.6(12)	-11.3(9)	7.9(8)	-3.6(8)
C(8)	48.3(11)	55.0(12)	55.8(11)	7.1(9)	3.0(9)	-4.6(9)
C(9)	41.5(10)	40.5(10)	75.4(14)	-3.4(9)	1.9(9)	-0.8(7)
C(10)	42(1)	55.3(11)	56.9(12)	-17.3(9)	7.0(8)	-3.1(8)
C(11)	42.3(10)	54.7(11)	53.7(11)	1.6(9)	5.6(8)	-6.2(8)
C(12)	44.6(10)	37.7(9)	66.4(13)	-2.6(8)	6.5(9)	-3.0(7)
C(13)	78.1(17)	95(2)	70.5(16)	-32.9(15)	12.1(13)	-3.1(15)
C(14)	81.7(18)	41.8(12)	140(3)	-2.2(14)	-1.4(18)	6.4(11)
C(15)	83.3(19)	102(2)	64.0(16)	23.2(15)	8.7(13)	-10.5(16)

Table S2d. Selected bond lengths for phase II of C₆H₃(CH₃)₃:C₆F₆.

Atom — Atom	Length / Å	Atom — Atom	Length / Å
C(1) — C(2)	1.359(3)	C(6) — F(6)	1.331(3)
C(1) — C(6)	1.360(3)	C(7) — C(8)	1.387(3)
C(1) — F(1)	1.339(3)	C(7) — C(12)	1.380(3)
C(2) — C(3)	1.359(4)	C(7) — C(13)	1.512(3)
C(2) — F(2)	1.330(3)	C(8) — C(9)	1.392(3)
C(3) — C(4)	1.390(5)	C(9) — C(10)	1.384(3)
C(3) — F(3)	1.332(3)	C(9) — C(14)	1.504(3)
C(4) — C(5)	1.376(5)	C(10) — C(11)	1.387(3)
C(4) — F(4)	1.333(3)	C(11) — C(12)	1.384(3)
C(5) — C(6)	1.356(4)	C(11) — C(15)	1.510(3)
C(5) — F(5)	1.337(3)		

Table S2e. Selected bond angles for phase II of C₆H₃(CH₃)₃:C₆F₆.

Atom — Atom — Atom	Angle / °	Atom — Atom — Atom	Angle / °
C(2) — C(1) — C(6)	121.2(2)	C(5) — C(6) — C(1)	119.7(3)
F(1) — C(1) — C(2)	119.9(2)	F(6) — C(6) — C(1)	119.7(3)
F(1) — C(1) — C(6)	118.9(2)	F(6) — C(6) — C(5)	120.6(3)
C(1) — C(2) — C(3)	119.9(2)	C(8) — C(7) — C(13)	120.8(2)
F(2) — C(2) — C(1)	119.3(2)	C(12) — C(7) — C(8)	118.34(19)
F(2) — C(2) — C(3)	120.7(2)	C(12) — C(7) — C(13)	120.9(2)
C(2) — C(3) — C(4)	119.5(3)	C(7) — C(8) — C(9)	121.3(2)
F(3) — C(3) — C(2)	119.8(3)	C(8) — C(9) — C(14)	120.7(2)
F(3) — C(3) — C(4)	120.7(3)	C(10) — C(9) — C(8)	118.51(19)
C(5) — C(4) — C(3)	119.4(2)	C(10) — C(9) — C(14)	120.8(2)
F(4) — C(4) — C(3)	119.5(4)	C(9) — C(10) — C(11)	121.51(19)
F(4) — C(4) — C(5)	121.1(4)	C(10) — C(11) — C(15)	121.2(2)
C(6) — C(5) — C(4)	120.2(3)	C(12) — C(11) — C(10)	118.3(2)
F(5) — C(5) — C(4)	119.1(3)	C(12) — C(11) — C(15)	120.5(2)
F(5) — C(5) — C(6)	120.6(3)	C(7) — C(12) — C(11)	122.06(19)

Table S3a. Crystal data and structure refinement for phase III of C₆H₃(CH₃)₃:C₆F₆.

Identification code	xstr0591b_new
Empirical formula	C ₁₅ H ₁₂ F ₆
Formula weight	306.25
Temperature / K	100
Crystal system	orthorhombic
Space group	Pb2 ₁ a [†]
<i>a</i> / Å	13.93854(8)
<i>b</i> / Å	15.18032(8)
<i>c</i> / Å	13.14822(7)
α / °	90
β / °	90
γ / °	90
Volume / Å ³	2782.05(3)
<i>Z</i>	8
ρ_{calc} / g cm ⁻³	1.462
μ/mm^{-1}	1.249
<i>F</i> (000)	1248.0
Crystal size / mm ³	0.873 × 0.615 × 0.408
Radiation	CuKα (λ = 1.54184)
2θ range for data collection/°	9.246 to 147.506
Index ranges	-17 ≤ <i>h</i> ≤ 17, -18 ≤ <i>k</i> ≤ 18, -16 ≤ <i>l</i> ≤ 16
Reflections collected	43732
Independent reflections	5558 [$R_{\text{int}} = 0.0250$, $R_{\text{sigma}} = 0.0105$]
Data/restraints/parameters	5558/1/385
Goodness-of-fit on <i>F</i> ²	1.081
Final <i>R</i> indexes [<i>I</i> >= 2σ(<i>I</i>)]	$R_1 = 0.0342$, $wR_2 = 0.0970$
Final <i>R</i> indexes [all data]	$R_1 = 0.0344$, $wR_2 = 0.0973$
Largest diff. peak/hole / e Å ⁻³	0.24/-0.28

[†]Space group chosen with the origin offset by (1/8, *y*, 1/4) from the 2₁-screw axis along *b* using the non-standard symmetry operators: *x*, *y*, *z* (1); 3/4 - *x*, 1/2 + *y*, *z* (*b*); 1/4 - *x*, 1/2 + *y*, 1/2 - *z* (2₁); and 1/2 + *x*, *y*, 1/2 - *z* (*a*). This unusual setting of the space group allows a direct comparison of the structure of phase III with phases I and II (as seen in Figure 3).

Table S3b. Fractional atomic coordinates ($\times 10^4$) and equivalent isotropic displacement parameters ($\text{\AA}^2 \times 10^3$) for phase III of $\text{C}_6\text{H}_3(\text{CH}_3)_3:\text{C}_6\text{F}_6$. U_{eq} is defined as $\frac{1}{3}$ of the trace of the orthogonalised U_{ij} tensor.

Atom	x	y	z	$U(\text{eq})$
C(1A)	5407.1(16)	6140.4(16)	3081.4(19)	29.6(5)
C(2A)	5518.5(17)	5400.1(18)	3669.4(18)	33.6(5)
C(3A)	5713(2)	4602.8(18)	3228(2)	40.4(6)
C(4A)	5798.4(18)	4545(2)	2190(3)	43.5(7)
C(5A)	5692.4(17)	5282(2)	1592.9(19)	38.7(6)
C(6A)	5493.7(18)	6085.5(18)	2043.4(18)	32.8(5)
F(1A)	5232.6(12)	6917.5(10)	3520.3(12)	42.7(4)
F(2A)	5442.5(13)	5468.9(13)	4684.6(11)	50.7(4)
F(3A)	5812.9(15)	3883.1(12)	3811.6(18)	67.8(6)
F(4A)	5986.6(13)	3764.8(13)	1762.7(19)	67.3(6)
F(5A)	5794.2(13)	5232.9(16)	585.7(12)	62.1(6)
F(6A)	5396.3(14)	6808.1(13)	1474.2(13)	53.7(5)
C(1B)	4594.8(16)	3260.3(17)	8417.4(18)	29.4(5)
C(2B)	4580.0(18)	3356(2)	7370.3(19)	33.6(5)
C(3B)	4383.7(18)	4170(2)	6960(2)	43.8(7)
C(4B)	4212.2(19)	4886(2)	7585(3)	46.7(8)
C(5B)	4225.8(18)	4780.2(19)	8620(3)	42.4(6)
C(6B)	4414.9(17)	3971.4(18)	9034.9(19)	33.5(5)
F(1B)	4769.1(12)	2471.8(10)	8823.7(12)	43.1(4)
F(2B)	4732.6(13)	2661.5(13)	6780.1(13)	51.2(4)
F(3B)	4358.1(13)	4264.3(18)	5955.4(14)	68.5(7)
F(4B)	4018.3(14)	5670.8(14)	7186(2)	73.4(7)
F(5B)	4036.1(14)	5465.9(12)	9238.7(18)	65.2(6)
F(6B)	4408.0(12)	3860.2(13)	10052.2(11)	48.4(4)
C(7A)	2993.1(16)	6010.5(17)	3804.8(18)	29.4(5)
C(8A)	3176.0(15)	5112.6(16)	3713.0(19)	29.4(5)
C(9A)	3228.1(16)	4704.6(16)	2769(2)	29.1(5)
C(10A)	3104.4(15)	5214.1(15)	1899.6(18)	27.6(5)
C(11A)	2917.8(15)	6114.2(16)	1962.4(19)	28.2(5)
C(12A)	2865.9(16)	6500.1(16)	2917.7(19)	28.6(5)
C(13A)	2939(2)	6441(2)	4835(2)	45.4(6)
C(14A)	3406(2)	3726.7(17)	2676(2)	42.3(6)
C(15A)	2793(2)	6659.7(19)	1015(2)	39.7(6)
C(7B)	2055.3(16)	3317.2(17)	8405.1(18)	29.5(5)
C(8B)	2155.2(16)	2942.2(16)	7444.8(18)	28.2(5)
C(9B)	2048.5(16)	3438.5(16)	6561.5(18)	29.4(5)
C(10B)	1848.0(16)	4334.5(16)	6654.0(18)	30.2(5)
C(11B)	1749.1(16)	4729.7(16)	7604(2)	30.5(5)
C(12B)	1852.9(16)	4214.5(17)	8469.5(19)	30.9(5)
C(13B)	2157(2)	2766(2)	9351(2)	44.7(6)

C(14B)	2153(2)	3013(2)	5532(2)	45.2(6)
C(15B)	1544(2)	5704.8(18)	7688(3)	48.1(7)
H(8A)	3265	4778	4298	35
H(10A)	3147	4949	1264	33
H(12A)	2743	7101	2967	34
H(13A)	2397	6212	5201	68
H(13B)	2869	7066	4754	68
H(13C)	3516	6318	5208	68
H(14A)	3631	3501	3315	63
H(14B)	3881	3622	2161	63
H(14C)	2820	3435	2493	63
H(15A)	2403	7164	1165	59
H(15B)	2487	6312	499	59
H(15C)	3409	6851	776	59
H(8B)	2297	2345	7392	34
H(10B)	1779	4675	6070	36
H(12B)	1786	4474	9106	37
H(13D)	2316	3140	9916	67
H(13E)	2657	2340	9253	67
H(13F)	1563	2469	9486	67
H(14D)	1783	3336	5042	68
H(14E)	1926	2417	5564	68
H(14F)	2816	3016	5335	68
H(15D)	2136	6020	7768	72
H(15E)	1141	5811	8268	72
H(15F)	1224	5903	7083	72

Table S3c. Anisotropic displacement parameters ($\text{\AA}^2 \times 10^3$) for phase III of $\text{C}_6\text{H}_3(\text{CH}_3)_3:\text{C}_6\text{F}_6$.Anisotropic displacement factor exponent has the form: $-2\pi^2[h^2a^{*2}U_{11}+2hka^{*}b^{*}U_{12}+\dots]$.

Atom	U_{11}	U_{22}	U_{33}	U_{23}	U_{13}	U_{12}
C(1A)	27.5(11)	30.1(12)	31.3(12)	-1.3(10)	0.5(9)	-1.1(9)
C(2A)	29(1)	42.0(14)	29.7(11)	6.6(11)	1.5(9)	-1.8(10)
C(3A)	30.9(12)	33.8(13)	56.5(17)	8.0(12)	-5.7(11)	3.7(10)
C(4A)	25.4(12)	36.6(14)	68.4(19)	-18.0(13)	-1.2(12)	4.1(10)
C(5A)	26.0(11)	58.8(17)	31.2(12)	-11.4(12)	2.3(9)	-7.0(11)
C(6A)	31.9(12)	37.8(13)	28.8(12)	8.2(10)	-2.4(9)	-7.4(10)
F(1A)	49.4(8)	34.1(8)	44.7(9)	-7.6(6)	-2.2(7)	3.4(7)
F(2A)	57.6(9)	65.9(11)	28.5(7)	11.4(7)	1.7(6)	-4.2(8)
F(3A)	71.8(12)	39.3(9)	92.5(15)	22(1)	-16.7(11)	6.6(9)
F(4A)	47.2(10)	52.2(11)	102.6(16)	-39.4(11)	-7.2(10)	11.4(8)
F(5A)	49.4(9)	104.5(17)	32.3(8)	-23.1(10)	4.8(7)	-16.9(10)
F(6A)	65.7(11)	54.2(11)	41.1(9)	21.9(8)	-10.7(8)	-13.6(8)
C(1B)	27.8(10)	31.7(11)	28.9(11)	4.1(9)	-2.3(9)	-4.1(9)
C(2B)	27.9(11)	42.7(14)	30.4(12)	0.0(11)	-1.3(9)	-8.2(10)
C(3B)	28.9(11)	65.7(19)	36.7(13)	21.9(13)	-5.5(9)	-10.1(12)
C(4B)	24.9(12)	42.8(17)	72(2)	23.5(15)	-3.8(12)	0.2(12)
C(5B)	27.3(11)	35.4(13)	64.5(18)	-1.4(13)	3.0(12)	3.1(10)
C(6B)	28(1)	40.4(13)	32.1(12)	-3.6(10)	1.2(9)	-2.5(9)
F(1B)	58.1(9)	32.6(8)	38.5(8)	6.4(6)	-0.6(7)	0.0(7)
F(2B)	57(1)	62.3(11)	34.3(8)	-15.7(8)	3.8(7)	-13.7(8)
F(3B)	55.6(10)	112.7(18)	37.0(9)	36.4(11)	-9.7(7)	-17.8(11)
F(4B)	49.9(10)	57.2(12)	113.2(18)	48.2(13)	-6.6(11)	5.5(9)
F(5B)	56.6(10)	39.7(9)	99.2(16)	-16.1(10)	11(1)	9.7(8)
F(6B)	57.2(9)	58.9(10)	29.1(7)	-8.5(7)	2.7(6)	-3.6(8)
C(7A)	23.6(10)	33.4(12)	31.3(12)	-2.8(10)	2.0(8)	-4.1(8)
C(8A)	24.5(9)	32.8(12)	30.8(11)	8.9(9)	-0.8(8)	0.7(9)
C(9A)	22.2(10)	24.3(11)	40.9(13)	2.1(9)	3.2(9)	-0.6(8)
C(10A)	25.3(10)	27.9(11)	29.5(11)	-1.6(9)	3.0(8)	-2.2(8)
C(11A)	22.5(10)	28.5(11)	33.7(12)	5.7(9)	2.2(8)	-0.8(8)
C(12A)	23.9(10)	21.6(10)	40.4(13)	0.4(9)	2.6(9)	-1.1(8)
C(13A)	46.8(15)	53.7(16)	35.6(13)	-11.9(12)	2.9(11)	-6.6(13)
C(14A)	41.3(14)	25.8(13)	59.8(17)	5.2(11)	9.0(12)	3.4(11)
C(15A)	43.5(13)	37.1(14)	38.3(13)	13.1(11)	2.5(11)	1.4(10)
C(7B)	25(1)	32.6(12)	31.0(12)	5.8(9)	-0.8(8)	-3.0(9)
C(8B)	27.4(11)	23.2(11)	34.2(12)	2.1(8)	0.9(9)	-1.4(9)
C(9B)	25.3(10)	33.1(13)	30.0(12)	-1.9(9)	0.4(8)	-4.4(9)
C(10B)	24.3(10)	32.3(12)	34.0(12)	8.9(9)	-0.5(8)	-2.4(9)
C(11B)	22.4(10)	23.9(11)	45.1(14)	0.8(9)	0.8(9)	-1.6(8)
C(12B)	26.4(10)	34.5(12)	32.0(12)	-4.4(10)	1.3(8)	-2.4(9)
C(13B)	43.4(14)	51.8(16)	39.0(14)	17.1(12)	-1.3(11)	-1.3(12)
C(14B)	50.1(15)	50.9(16)	34.6(13)	-9.6(12)	4.6(11)	-7.8(12)
C(15B)	42.1(14)	25.5(12)	77(2)	-2.4(13)	5.7(13)	1.8(11)

Table S3d. Selected bond lengths for phase III of C₆H₃(CH₃)₃:C₆F₆.

Atom — Atom	Length / Å	Atom — Atom	Length / Å
C(1A) — C(2A)	1.373(3)	C(5B) — C(6B)	1.369(4)
C(1A) — C(6A)	1.373(4)	C(5B) — F(5B)	1.347(3)
C(1A) — F(1A)	1.336(3)	C(6B) — F(6B)	1.348(3)
C(2A) — C(3A)	1.370(4)	C(7A) — C(8A)	1.392(3)
C(2A) — F(2A)	1.343(3)	C(7A) — C(12A)	1.394(3)
C(3A) — C(4A)	1.372(5)	C(7A) — C(13A)	1.506(3)
C(3A) — F(3A)	1.342(3)	C(8A) — C(9A)	1.389(4)
C(4A) — C(5A)	1.375(5)	C(9A) — C(10A)	1.391(4)
C(4A) — F(4A)	1.337(3)	C(9A) — C(14A)	1.510(3)
C(5A) — C(6A)	1.384(4)	C(10A) — C(11A)	1.393(3)
C(5A) — F(5A)	1.334(3)	C(11A) — C(12A)	1.388(4)
C(6A) — F(6A)	1.335(3)	C(11A) — C(15A)	1.506(3)
C(1B) — C(2B)	1.385(4)	C(7B) — C(8B)	1.392(3)
C(1B) — C(6B)	1.374(4)	C(7B) — C(12B)	1.394(4)
C(1B) — F(1B)	1.333(3)	C(7B) — C(13B)	1.505(3)
C(2B) — C(3B)	1.375(4)	C(8B) — C(9B)	1.392(3)
C(2B) — F(2B)	1.326(3)	C(9B) — C(10B)	1.394(3)
C(3B) — C(4B)	1.383(5)	C(9B) — C(14B)	1.506(3)
C(3B) — F(3B)	1.329(3)	C(10B) — C(11B)	1.392(4)
C(4B) — C(5B)	1.371(5)	C(11B) — C(12B)	1.389(4)
C(4B) — F(4B)	1.330(3)	C(11B) — C(15B)	1.512(4)

Table 3e. Selected bond angles for phase III of C₆H₃(CH₃)₃:C₆F₆.

Atom — Atom — Atom	Angle / °	Atom — Atom — Atom	Angle / °
C(6A) — C(1A) C(2A)	120.0(2)	C(6B) — C(5B) C(4B)	120.2(3)
F(1A) — C(1A) C(2A)	120.0(2)	F(5B) — C(5B) C(4B)	120.4(3)
F(1A) — C(1A) C(6A)	119.9(2)	F(5B) — C(5B) C(6B)	119.4(3)
C(3A) — C(2A) C(1A)	120.5(2)	C(5B) — C(6B) C(1B)	120.3(2)
F(2A) — C(2A) C(1A)	119.1(2)	F(6B) — C(6B) C(1B)	119.3(2)
F(2A) — C(2A) C(3A)	120.4(2)	F(6B) — C(6B) C(5B)	120.4(2)
C(2A) — C(3A) C(4A)	119.7(2)	C(8A) — C(7A) C(12A)	118.2(2)
F(3A) — C(3A) C(2A)	119.8(3)	C(8A) — C(7A) C(13A)	120.8(2)
F(3A) — C(3A) C(4A)	120.5(3)	C(12A) — C(7A) C(13A)	121.0(2)
C(3A) — C(4A) C(5A)	120.4(2)	C(9A) — C(8A) C(7A)	121.6(2)
F(4A) — C(4A) C(3A)	119.5(3)	C(8A) — C(9A) C(10A)	118.7(2)
F(4A) — C(4A) C(5A)	120.1(3)	C(8A) — C(9A) C(14A)	121.3(2)
C(4A) — C(5A) C(6A)	119.6(2)	C(10A) — C(9A) C(14A)	120.0(2)
F(5A) — C(5A) C(4A)	120.7(3)	C(9A) — C(10A) C(11A)	121.3(2)
F(5A) — C(5A) C(6A)	119.7(3)	C(10A) — C(11A) C(15A)	120.8(2)
C(1A) — C(6A) C(5A)	119.8(2)	C(12A) — C(11A) C(10A)	118.5(2)
F(6A) — C(6A) C(1A)	119.9(2)	C(12A) — C(11A) C(15A)	120.7(2)
F(6A) — C(6A) C(5A)	120.3(2)	C(11A) — C(12A) C(7A)	121.7(2)
C(6B) — C(1B) C(2B)	120.2(2)	C(8B) — C(7B) C(12B)	118.4(2)
F(1B) — C(1B) C(2B)	119.7(2)	C(8B) — C(7B) C(13B)	120.8(2)
F(1B) — C(1B) C(6B)	120.1(2)	C(12B) — C(7B) C(13B)	120.8(2)
C(3B) — C(2B) C(1B)	119.2(3)	C(7B) — C(8B) C(9B)	121.6(2)
F(2B) — C(2B) C(1B)	119.7(3)	C(8B) — C(9B) C(10B)	118.5(2)
F(2B) — C(2B) C(3B)	121.1(2)	C(8B) — C(9B) C(14B)	120.5(2)
C(2B) — C(3B) C(4B)	120.4(3)	C(10B) — C(9B) C(14B)	121.0(2)
F(3B) — C(3B) C(2B)	119.5(3)	C(11B) — C(10B) C(9B)	121.2(2)
F(3B) — C(3B) C(4B)	120.0(3)	C(10B) — C(11B) C(15B)	120.5(3)
C(5B) — C(4B) C(3B)	119.7(3)	C(12B) — C(11B) C(10B)	118.8(2)
F(4B) — C(4B) C(3B)	120.3(3)	C(12B) — C(11B) C(15B)	120.7(3)
F(4B) — C(4B) C(5B)	119.9(3)	C(11B) — C(12B) C(7B)	121.4(2)

Table S4. Lattice parameter data obtained from whole pattern fitting to the data shown in Figure 1 (and Figure S1).

<i>T / K</i>	<i>a / Å</i>	<i>b / Å</i>	<i>c / Å</i>	$\beta / {}^\circ$	<i>V / Å³</i>
300	7.1749(4)	15.5935(6)	13.4988(12)	90	1510.3(2)
290	7.1636(4)	15.5675(6)	13.4810(10)	90	1503.4(1)
280	7.1533(3)	15.5405(5)	13.4634(8)	90	1496.7(1)
270	7.1414(2)	15.5129(4)	13.4422(6)	90	1489.2(1)
260	7.1302(2)	15.4869(4)	13.4233(6)	90	1482.3(1)
250	7.1196(2)	15.4620(4)	13.4046(6)	90	1475.6(1)
240	7.1103(2)	15.4365(4)	13.3859(7)	90	1469.2(1)
230	7.1017(2)	15.4107(4)	13.3675(7)	90	1463.0(1)
220	7.0941(2)	15.3863(4)	13.3480(7)	90	1457.0(1)
210	7.0865(2)	15.3622(4)	13.3279(8)	90	1450.9(1)
200	7.0784(3)	15.3390(3)	13.3098(8)	90	1445.1(1)
190	7.0713(3)	15.3171(3)	13.2916(8)	90	1439.6(1)
180	7.0649(3)	15.2958(3)	13.2735(8)	90	1434.4(1)
170	7.1023(5)	15.2924(3)	13.2884(14)	96.453(10)	1434.1(2)
160	7.0967(5)	15.2882(3)	13.2490(8)	96.247(6)	1428.9(1)
150	7.0757(4)	15.2806(3)	13.2118(5)	96.587(5)	1419.0(1)
140	7.0699(3)	15.2708(3)	13.1957(4)	97.036(6)	1413.9(1)
130	7.0587(3)	15.2609(3)	13.1783(6)	97.478(7)	1407.5(1)
120	7.0619(4)	15.2505(3)	13.1606(4)	97.942(6)	1403.8(1)
110	7.0600(3)	15.2404(3)	13.1444(4)	98.291(6)	1399.5(1)
100	13.9687(2)	15.1880(4)	13.1350(9)	90	2786.7(4)
90	13.9487(2)	15.1752(3)	13.1244(7)	90	2778.1(4)

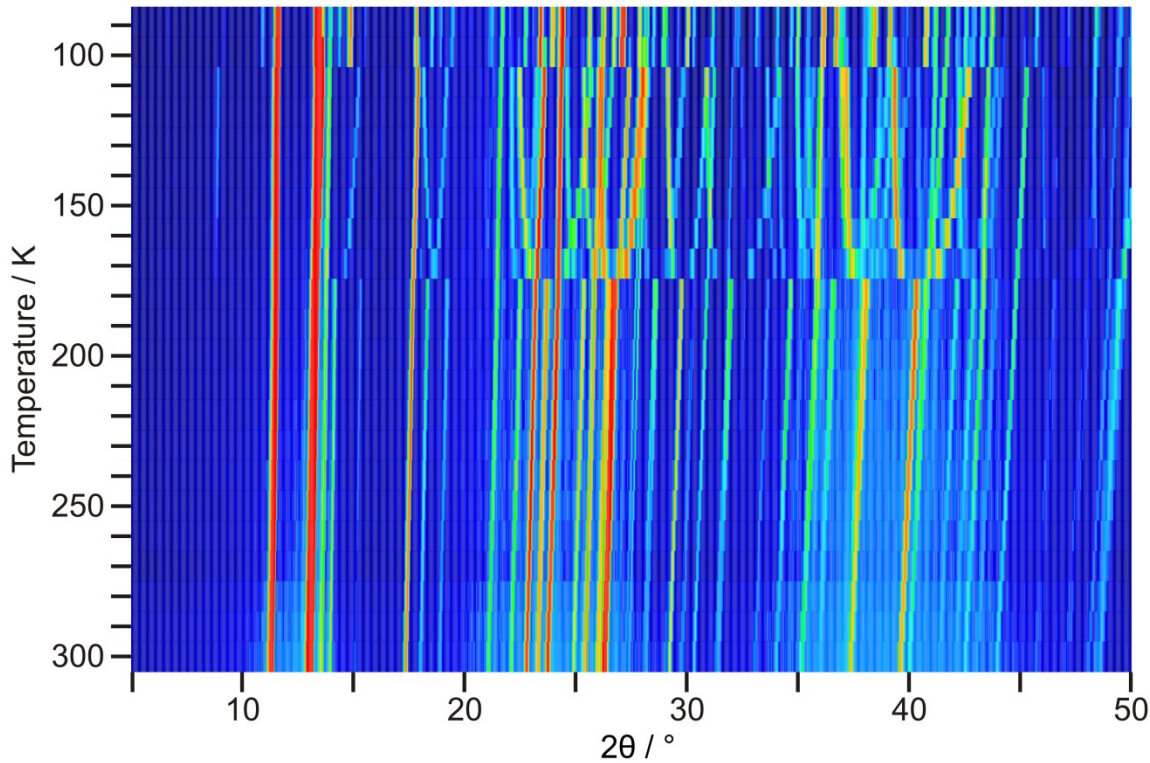


Figure S1. PXRD data collected on cooling a sample of $\text{C}_6\text{H}_3(\text{CH}_3)_3:\text{C}_6\text{F}_6$ from 300 K down to 90 K displayed as a thermo-diffractogram. X-ray intensity is shown using a thermal-style color scale going from blue (low intensity) via green and yellow to red (high intensity). The transition from $\text{C}_6\text{H}_3(\text{CH}_3)_3:\text{C}_6\text{F}_6$ phase I to phase II between 180 K and 170 K is clearly evident as is the transition from phase II to phase III between 110 K and 100 K.

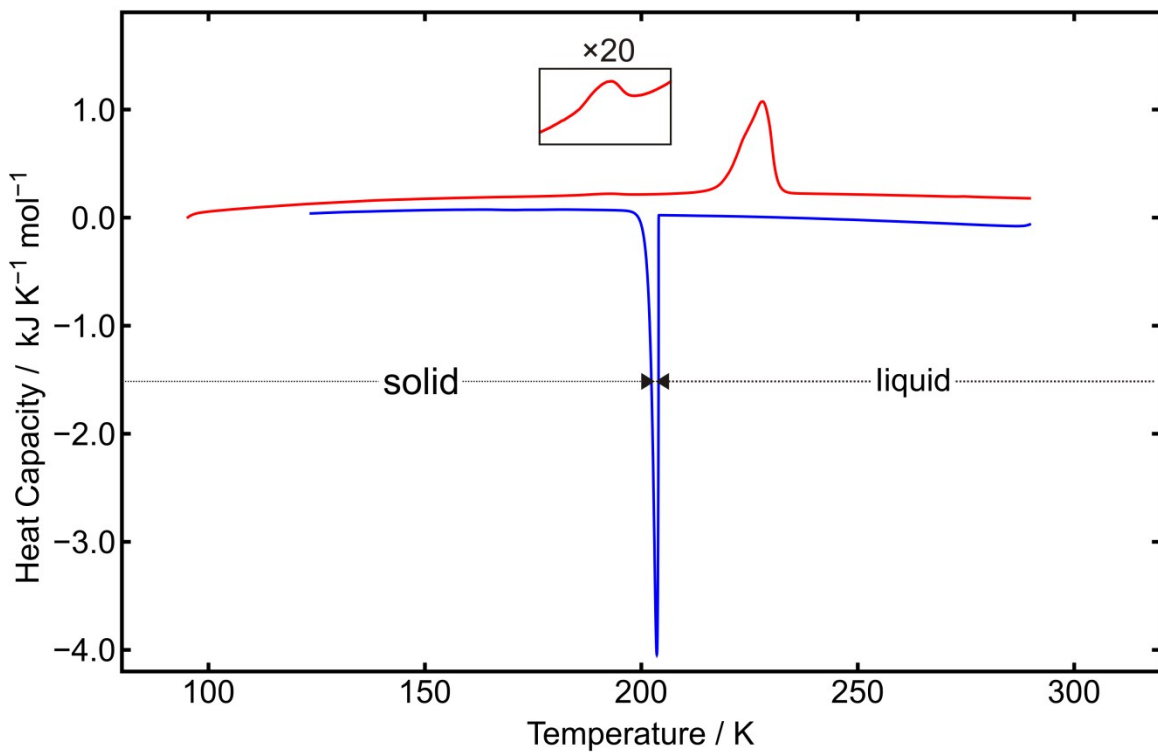


Figure S2. DSC data for pure mesitylene measured using the same procedure as for the binary adduct. The scan on pure mesitylene confirmed our suspicions of a surplus of mesitylene in the binary mixture caused by preferential loss through evaporation of the more volatile hexafluorobenzene. The insert shows a small pre-melting feature which may indicate that solid mesitylene exhibits an order-disorder transition just below the melting point.

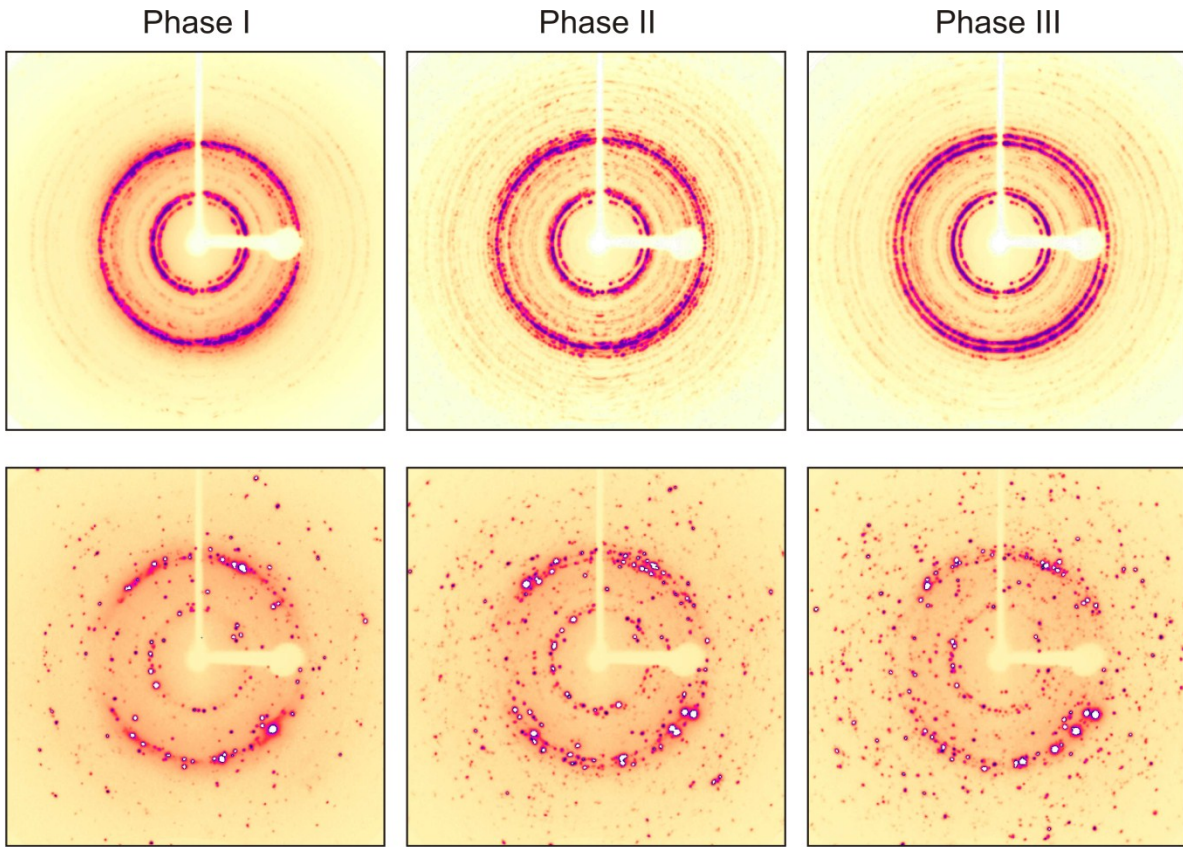


Figure S3. One of the issues in measuring samples frozen from the liquid state into X-ray capillaries is that the sample may contain relatively large crystallites and so exhibit sample granularity. Consequently, the intensities measured in a PXRD experiment with a 1-D detector may not be representative of an ideal powder sample, which is assumed to contain many small randomly-oriented crystallites. An experiment using a SXD diffractometer shows the effect of freezing a 1:1 molar mixture of C_6F_6 and 1,3,5- $C_6H_3Me_3$ into a 1 mm X-ray capillary and then measuring it as a function of temperature and phi-axis sample rotation on an Agilent Technologies SuperNova equipped with $Cu K\alpha_{12}$ radiation and an Atlas (135 mm) CCD detector. Diffraction images were collected of the capillary rotated by 180° for 180 s (top row) and of the stationary capillary for 5s (bottom row) as a function of temperature (phase I at 300 K, phase II at 150 K, and phase III at 90 K).

It is often erroneously believed that taking such a “powder” sample through one or more phase transitions will always produce a better powder due to the crystallites breaking up with each transition. Although this may work for some samples, it clearly did not work for this sample as evidenced by these images.

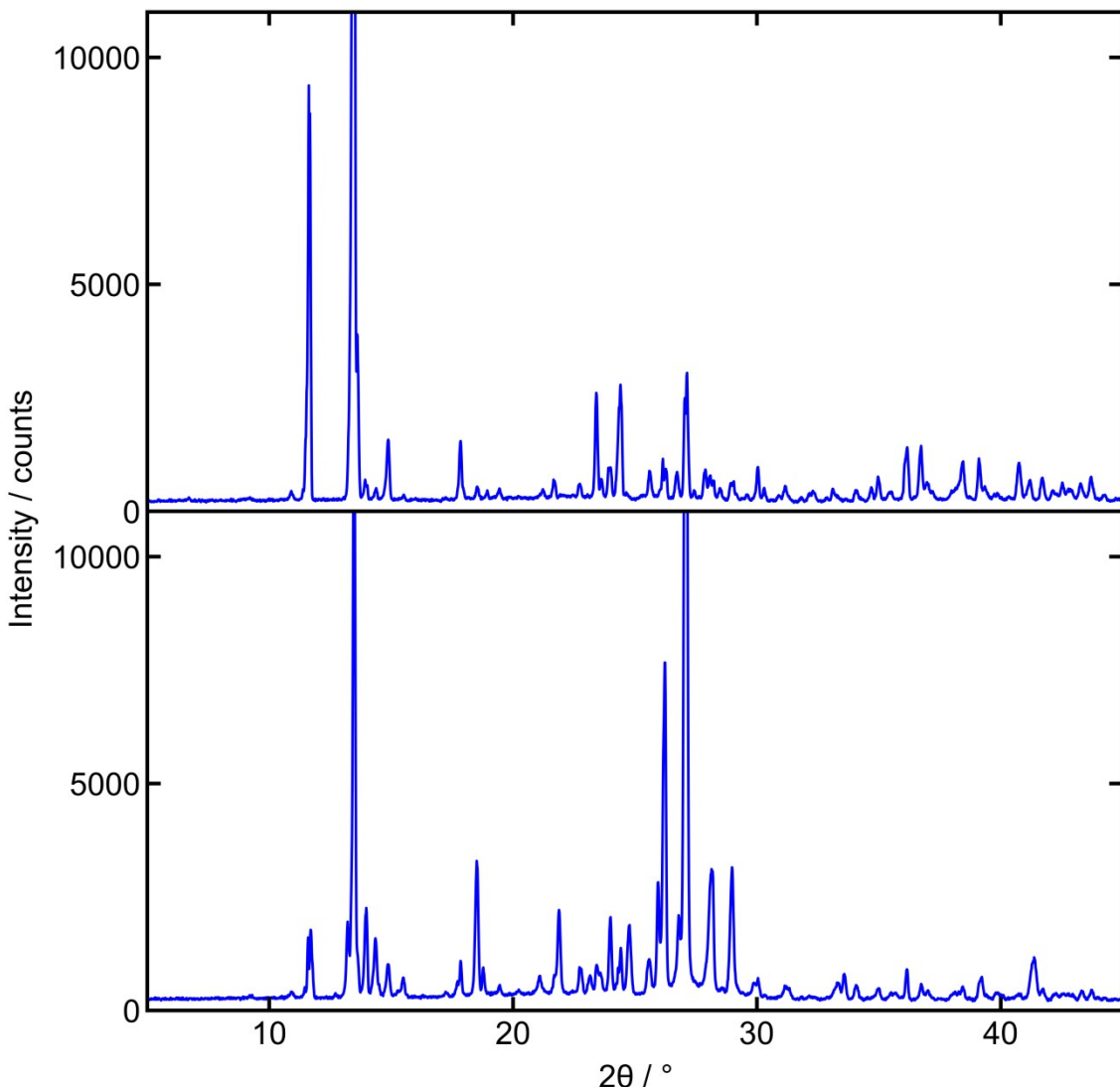


Figure S4. PXRD data were collected on a sample of $\text{C}_6\text{H}_3(\text{CH}_3)_3:\text{C}_6\text{F}_6$ at 100 K (upper). Subsequently, the experiment was repeated at the same temperature with a second sample from the same batch of material (lower). Although the peaks are observed at the same 2θ positions within experimental error, the experiment showed that, in this particular instance, the intensities are unreliable, though the data can be used to show phase transitions and for lattice parameter determination. Based on a single one-off PXRD measurement with a 1-D detector as typically used in most PXRD diffraction setups, there is no indication of the reliability of the measured X-ray diffraction intensities. However, repeat experiments using one or more samples, experiments using different PXRD geometries (e.g. Bragg-Brentano reflection with a flat-plate, X-ray transmission through a thin-foil or a capillary), and experiments with a 2-D detector (v.s. Figure S3) can all be used to monitor the effect of possible sample texture (i.e. sample granularity and/or preferred orientation) on the measured X-ray diffraction intensities.

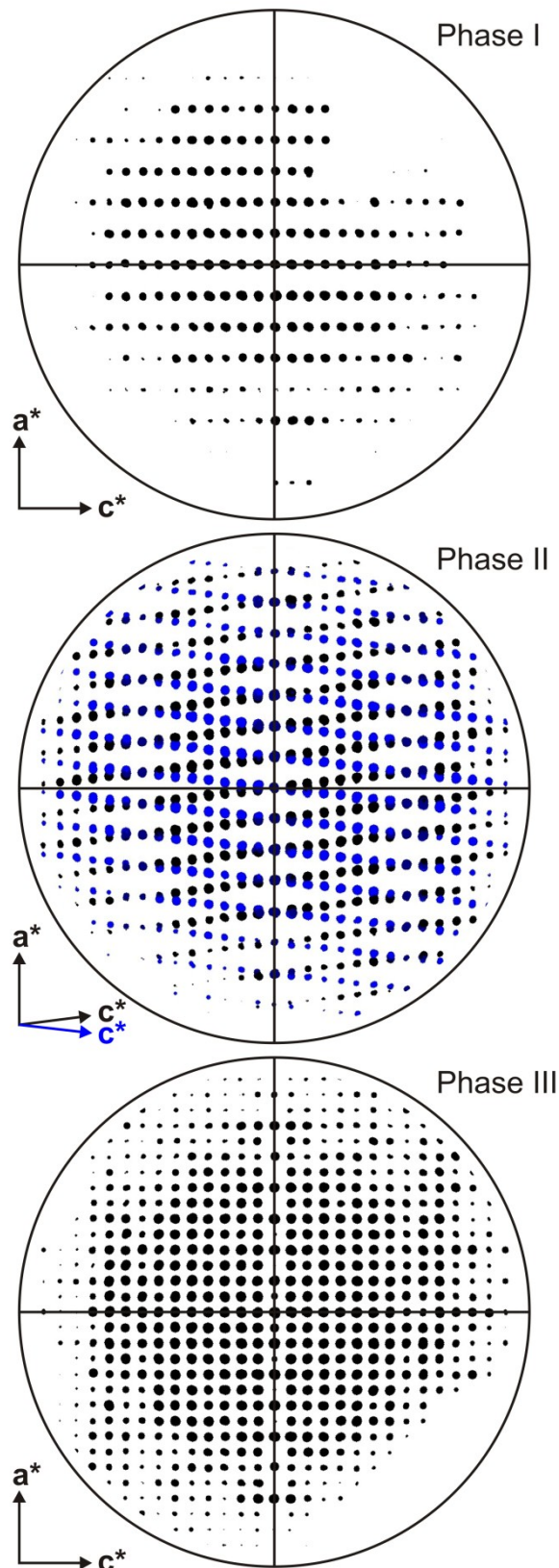


Figure S5. Single-crystal data plotted as a projection in reciprocal space viewed down \mathbf{b}^* showing the orthorhombic symmetry in phase I, the monoclinic symmetry in phase II with the two sets of spots (blue versus black) due to twinning, and the return to orthorhombic symmetry with a doubled unit cell in the lowest temperature phase. Figures generated with the Ewald Explorer option within CrysAlisPro.

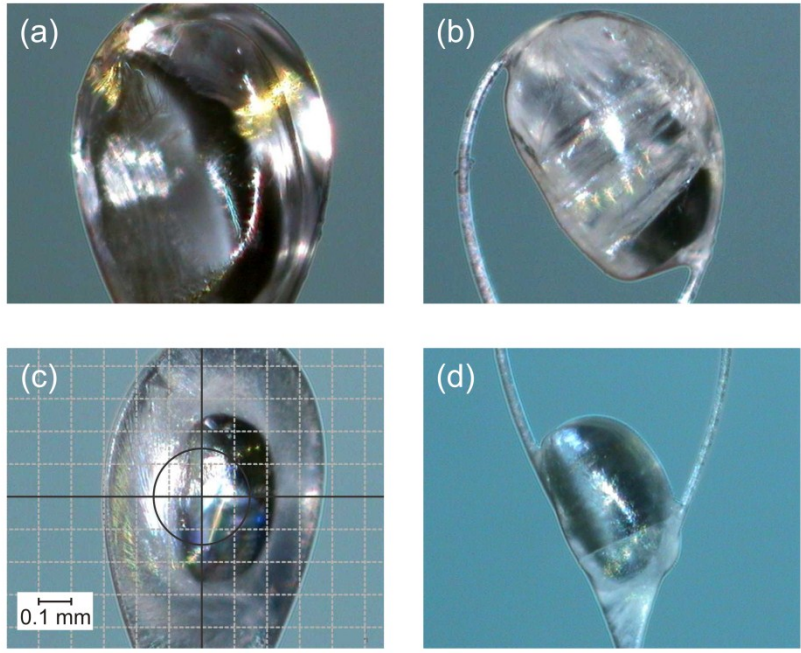
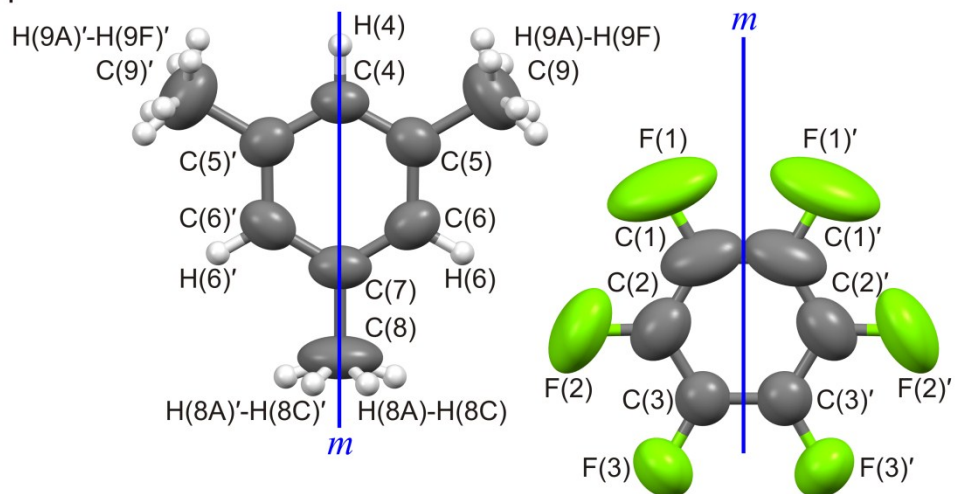
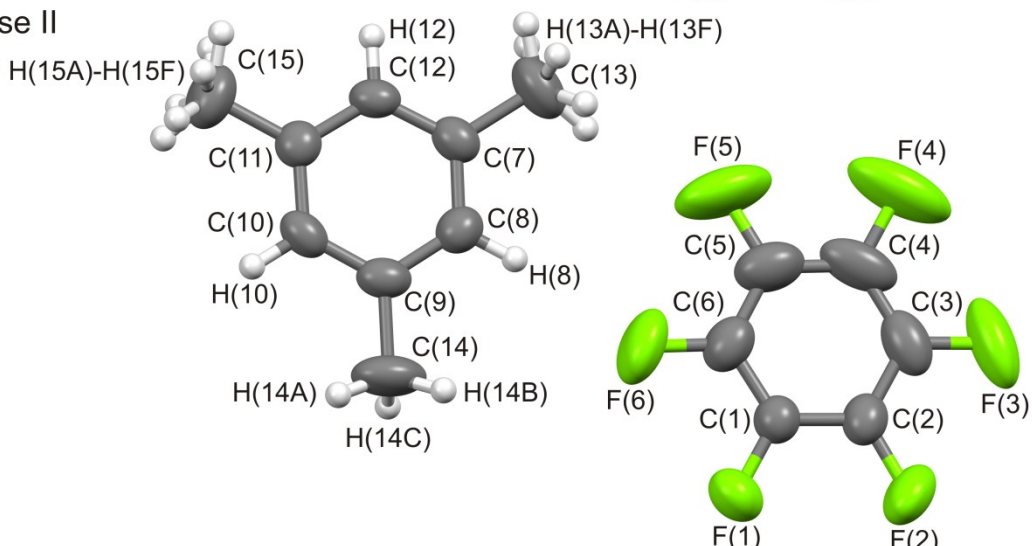


Figure S6. Views of the crystals of the binary adduct used in the single-crystal diffraction results reported here. An initial SXD experiment at 220 K with the crystal shown in (a) was unsuccessful due to sublimation of the crystal in the cold nitrogen flow of the Cryojet5. After a couple of hours it appeared as seen in (b). The temperature was then reduced to 190 K and further measurements made on phase I. Another set of measurements on this crystal was then made at 100 K when, serendipitously, the spots appeared to correspond to a single crystal as seen in Figure S5 (phase III), phase II not being measured at this point in time as its existence was then unknown. In a subsequent experiment, a second crystal was deliberately reduced in size via sublimation at about 250 K leaving it held in a film of frozen mesitylene on cooling to 150 K as seen in (c). The crystal was subsequently warmed back to phase I, the excess mesitylene removed as seen in (d), and re-cooled to 150 K to measure phase II as a 50:50 twin. Additional SXD measurements were made to confirm the thermal stabilities of the crystals on passing through the phase transitions including collection of several partial spheres of X-ray diffraction data on phase I.

Phase I



Phase II



Phase III

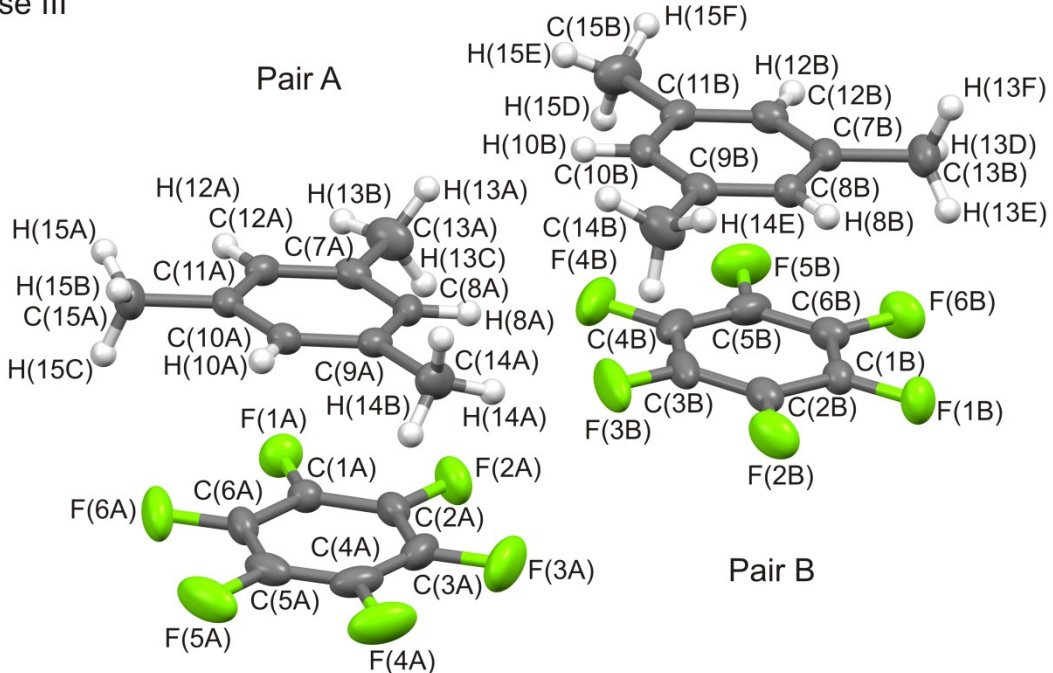


Figure S7. Labelling scheme used for the atoms in the refinement of the three crystal structures of $\text{C}_6\text{H}_3(\text{CH}_3)_3:\text{C}_6\text{F}_6$. Atoms labelled with a prime ('') in phase I are related by mirror symmetry m . (A few hydrogen atom labels for phase III have been omitted for clarity.)

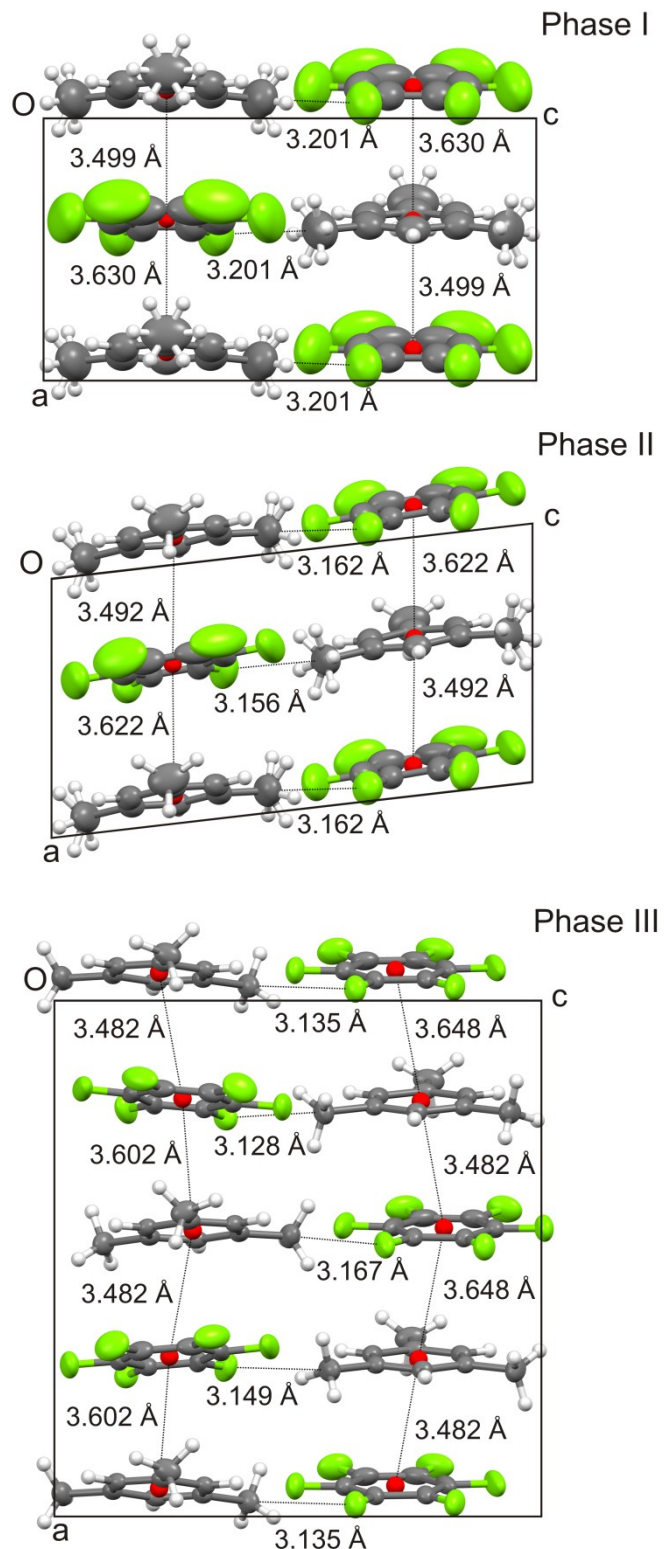


Figure S8. View of the crystal structures of $C_6H_3(CH_3)_3:C_6F_6$ seen down the b-axis for phase I (top), phase II (middle), and phase III (bottom) showing distances between ring centroids (shown in red) and the $-F \cdots H_3C-C$ bond distances (with s.u. on all lengths equal to 0.003 \AA). All crystal structure drawings in this paper were prepared using images from the program Mercury (version 3.7) obtainable from the Cambridge Crystallographic Data Centre and CorelDraw (version X3). Mean atomic-displacement parameters are shown as ellipsoids at the 50% probability level; C, F, and H atoms types are drawn in grey, green, and white, respectively.

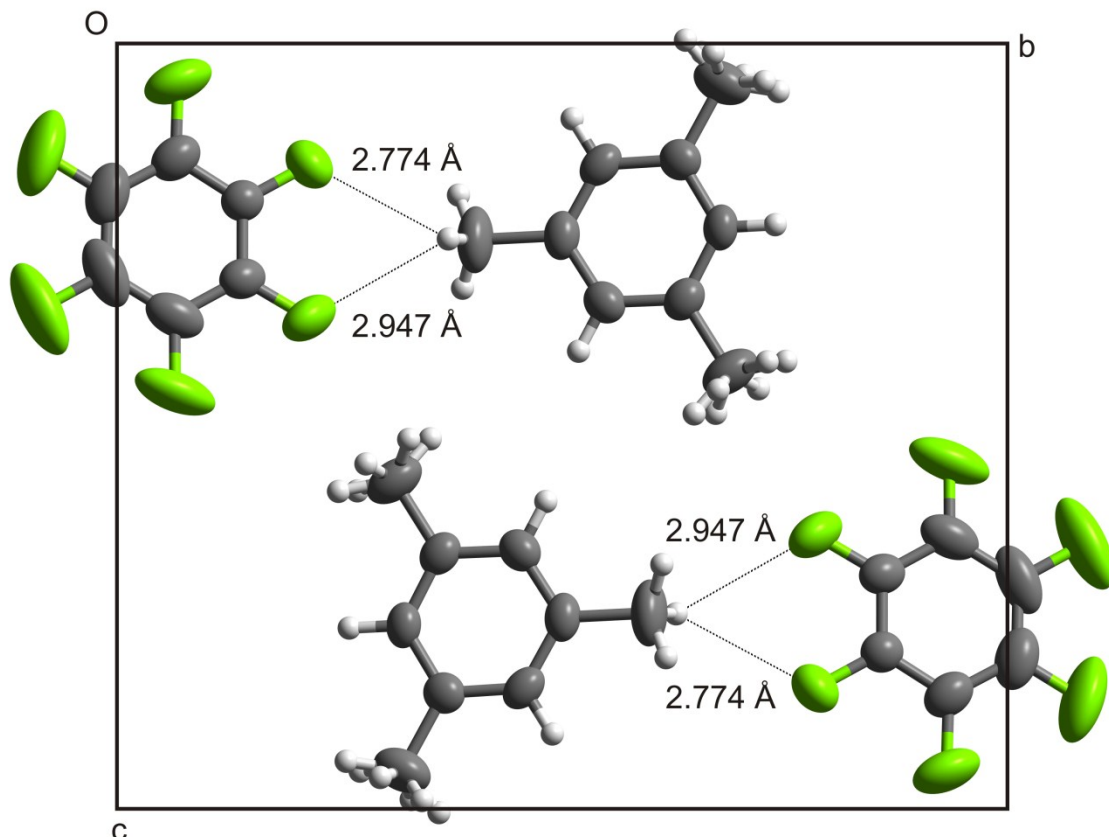


Figure S9. View of the crystal structure of $\text{C}_6\text{H}_3(\text{CH}_3)_3:\text{C}_6\text{F}_6$ seen down the a -axis showing the $\text{C}-\text{F}\dots\text{H}_3\text{C}-\text{C}$ interaction and the corresponding $\text{F}\dots\text{H}$ distances for the ordered methyl group in phase II. Our interpretation of the interaction of molecules in adjacent columns is based on approximating the interactions of bond-dipole moments; in particular, the $\text{C}-\text{F}$ and $\text{C}-\text{H}$ or $\text{C}-\text{CH}_3$ bond dipoles moments. Hexafluorobenzene has no overall dipole moment but any one of the six $\text{C}-\text{F}$ bonds has an appreciable separation of charge, which will be able to couple with another nearby bond-dipole moment. For example, we may approximate the bond-dipole moment in a hexafluorobenzene to be $\mu_{\text{C}-\text{F}}$ where μ is the ratio of the electronegativities of C and F . Likewise, we may approximate the bond-dipole moment in the methyl group of mesitylene as the ratio of the electronegativities of C and H , and two such bond-dipole moments will have a force of interaction proportional to $1/r^3$, where r is the distance between the centroids of the bonds [A. D. Buckingham, *Adv. Chem. Phys.* 1967, **12**, 107-142].

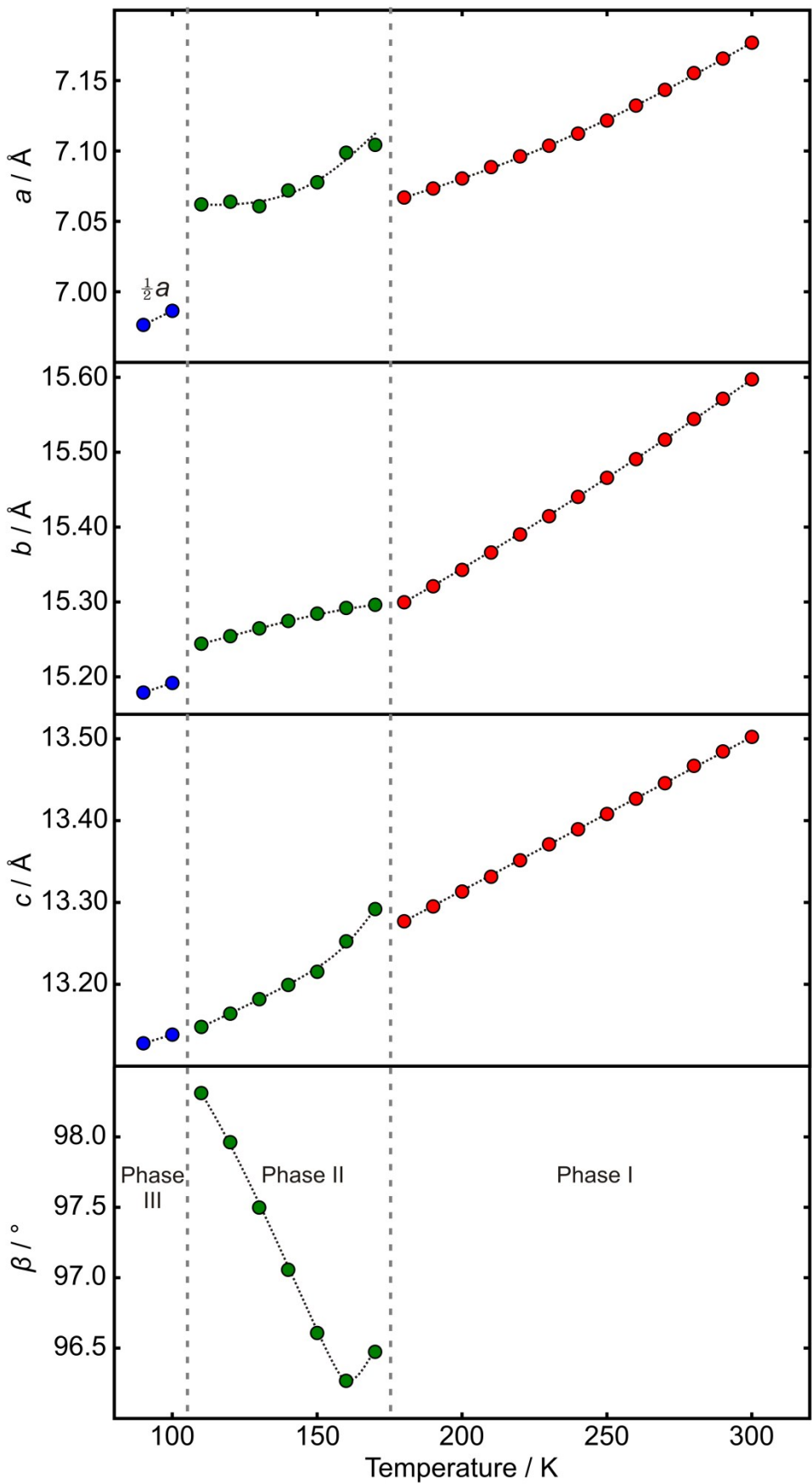


Figure S10. Lattice parameters shown as a function of T (from data in Table S4). Statistical errors from data fitting are smaller than the size of the points used.